Determination of corrugation and friction of Cu(111) toward adsorption and motion of Ne and Xe

Y. N. Zhang,[1,2,3,*] V. Bortolani,[3,4] and G. Mistura[5]

[1]*Chengdu Green Energy and Green Manufacturing Technology R&D Center, Sichuan, 620107, China*

[2]*Beijing Computational Science Research Center, Beijing, 100084, China*

[3]*Department of Physics and Astronomy, University of California, Irvine, California 92697, USA*

[4]*Dipartimento di Fisica, Università di Modena e Reggio Emilia, Via Campi 213/A, Modena, 41100 Italy*

[5]*Dipartimento di Fisica e Astronomia "G. Galilei" and CNISM, Universita di Padova, Via Marzolo 8, I-35131 Padova, Italy*

(Received 24 January 2014; revised manuscript received 20 March 2014; published 17 April 2014)

The corrugation feature of potential energy surfaces (PESs) for rare-gas (RG) adlayers on metal surfaces has been extensively explored in the positive adsorption energy part. Here, we show that opposite corrugation features may also happen in the negative adsorption energy side for Ne and Xe on Cu(111). While the PES of Ne/Cu(111) is corrugated near the equilibrium adsorption geometry, i.e., Ne prefers the hollow site, the PES of Xe/Cu(111) is anticorrugated, i.e., Xe prefers the atop site. The weak hybridization of RG p and Cu d states is critical for this qualitative difference. Furthermore, the calculated activation energies indicate that Ne may move on Cu(111) at a very low temperature, whereas Xe motion can be activated only above 35 K. We found that the inclusion of the nonlocal van der Waals correction is essential for the correct determination of adsorption and motion energetics for RG adatoms on metals through density functional calculations.

DOI: 10.1103/PhysRevB.89.165414 PACS number(s): 68.35.Af, 68.43.Bc, 71.15.Nc

I. INTRODUCTION

The interaction between a rare gas (RG) and a metal surface is typically described as the sum of two contributions: van der Waals attraction at large RG-metal distances, proportional to z^{-3}, and Pauli repulsion at short distances [1,2]. This gives rise to two important topics involving RG-substrate interactions in surface science. Considerations of RG within a repulsive (or positive adsorption energy) range give information on the surface dynamics, for example, regarding surface phonons and energy dissipation. On the other hand, one can detect the physisorption and frictional properties of RG on metal surfaces within the attractive (or negative adsorption energy) range. Fundamentally, the RG-metal interaction represents the weakest "bond" between two elements and still remains as a challenge for quantitative understanding, especially through density functional theory (DFT) calculations.

In the repulsive region, RG atoms can see either a corrugated or anticorrugated surface, depending on the charge density profile and electronic feature, as recognized a long time ago by Rieder *et al.* [3]. In the corrugated case, the scattering data can be described by a pair potential of the Esbjerg-Nørskov type [4], and as expected, the minimum distance of RG to surface (classical turning point) is over the high-coordination hollow site. In contrast, the turning point occurs at the low-coordination atop site on anticorrugated surfaces. Extensive theoretical studies, often with a tremendous number of parameters and some approximations, have been performed to understand the origin of the corrugation effect [5,6]. For example, Petersen *et al.* [7] provided descriptions on the interaction potentials of He and Ne with Rh(110) through DFT studies and convincingly explained experimental results.

The attraction between RG adatoms and metal substrates in the negative energy part is a subject of growing importance in the recent decades. Theoretically, many studies have touched on the adsorption geometry, tribological property, local hydrodynamic pressure, and electronic states of RG on surfaces [8–11], giving insights into the mechanism behind experimental observations. However, as far as we know, the corrugation and anticorrugation features of potential energy surfaces (PESs) near the equilibrium geometries have seldom been discussed. It is interesting and also important to explore these features of specific RG-metal systems since the corrugated or anticorrugated PES determines their bonding and gliding properties for practical applications. In addition, it has been recognized that DFT results of adsorption sites, adsorption energies, and activation energies can be significantly affected by the van der Waals (vdW) interactions, which are missing in most conventional DFT studies [12–16]. It is therefore of fundamental interest to carefully examine the effect of the vdW correction on the DFT description for weak RG-metal bonds, as we did previously for RG on Pb(111) [17].

In this paper, we report results of DFT calculations with the inclusion of nonlocal vdW correlation for the study of the surface properties of Ne and Xe monolayers on the Cu(111) surface. One major finding of this work is that opposite corrugation effects between Ne and Xe manifest in the negative adsorption energy region. Analyses on projected density of states and other electronic properties reveal that the hybridization between RG p states and Cu d states is the key reason for the determination of the corrugation feature. The activation energies for the sliding motion of Ne and Xe on Cu(111) and Pb(111) are also calculated for the understanding of their different tribological behaviors.

II. COMPUTATIONAL DETAILS

Density functional calculations were performed using the Vienna *Ab initio* Simulation Package (VASP) [18] along with projector-augmented wave (PAW) pseudopotentials [19]. We treated the exchange-correlation interaction among electrons with the optB86b version of the nonlocal vdW density functional (vdW-DF) [20–22]. The calculated lattice constant for

*yanningz@csrc.ac.cn

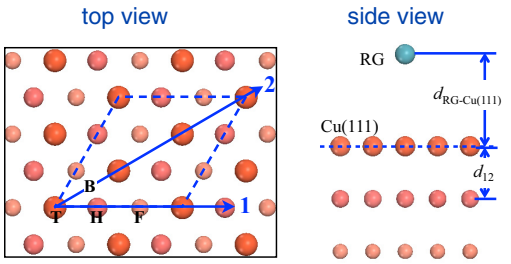

FIG. 1. (Color online) The top and side views of the atomic model adopted in the present calculations. Parallelogram in (a) shows the $\sqrt{3} \times \sqrt{3}$ unit cell, and the arrows 1 and 2 represent the two paths of RG sliding. The T, B, H, and F are for atop, bridge, hcp hollow, and fcc hollow sites, respectively. The large, medium, and small spheres are for the surface, subsurface, and third-layer Cu atoms, and notations $d_{RG\text{-}Cu(111)}$ and d_{12} are marked for the convenience of discussions.

the bulk Cu is 3.599 Å, in close agreement with experiments of 3.595 Å. We used a $(11 \times 11 \times 1)$ Monkhorst-Pack k-point grid to sample the two-dimensional Brillouin zone (BZ). An energy cutoff of 700 eV was adopted for the basis expansion. To simulate RG/Cu(111), we used a periodic model with a seven-layer slab for Cu(111) and an ~20-Å-thick vacuum in between. The RG monolayer was represented by a $(\sqrt{3} \times \sqrt{3})R30°$ lattice of RG adatoms on the Cu(111) substrate in the lateral plane, as depicted in Fig. 1; the lattice mismatch between Xe and Cu in this model is thus <0.1%. We fully optimized positions of RG adatoms along with the top five Cu layers and fixed the two bottommost Cu layers at their bulk positions.

III. RESULTS AND DISCUSSIONS

We first determined the ground state adsorption geometries of Ne and Xe on the Cu(111) surface by calculating their adsorption energies, E_{ad}, at the high-symmetric atop site, hexagonal close-packed (hcp) and face-centered-cubic (fcc) hollows, as well as the bridge site, as depicted in Fig. 1(a). Here, E_{ad} is defined by $E_{ad} = E_{tot} - E_{Cu(111)} - E_{RG\text{-}ML}$, with E_{tot}, $E_{Cu}(111)$, and $E_{RG\text{-}ML}$ representing total energies of RG/Cu(111), clean Cu(111), and isolated RG monolayer, respectively. The calculated values of E_{ad} and $d_{RG\text{-}Cu(111)}$ of all four configurations are listed in Table I. We found that for Ne/Cu(111), the E_{ad} values at the bridge and hollow sites are very close to each other and lower than that at the atop site. In contrast, Xe favors the low-coordination atop site, which is consistent with experimental observation using the low-energy electron diffraction [23] and with previous theoretical studies [12,24–28]. The results of E_{ad} indicate that in the ground state, the PES of Ne/Cu(111) is *corrugated*, but that of Xe/Cu(111) is *anticorrugated*. Quantitatively, the best E_{ad} of Ne/Cu(111) is only 51.0 meV, i.e., much lower than that of Xe/Cu(111), which is 280.5 meV. The distance between Ne and the Cu(111) surface, $d_{Ne\text{-}Cu(111)}$, is 3.44 Å, which is shorter than the corresponding $d_{Xe\text{-}Cu(111)}$ of 3.57–3.59 Å due to the smaller size of Ne. The adsorbate-induced substrate rumpling and the change of d_{12} are negligible [$\Delta d_{12} < 0.001$ Å for Ne/Cu(111) and $\Delta d_{12} < 0.005$ Å for Xe/Cu(111)].

To better appreciate the different behaviors of Ne and Xe on Cu(111), their adsorption energies over the top and hollow sites of Cu(111) are plotted in Fig. 2 against the interplanar distance. As expected from data in Table I, the potential wells of Xe/Cu(111) are significantly deeper than those of Ne/Cu(111). While the Ne-Cu interaction becomes negligible at a distance of ~5.7 Å, E_{ad} of Xe/Cu(111) still remains appreciable much beyond this point, indicating that the vdW force between Xe and Cu extends to a rather long range. The magnified view of E_{ad}–$d_{RG/Cu}(111)$ curves in Fig. 2(b) indicates that the PES of Ne/Cu(111) is *corrugated* around the equilibrium $d_{Ne/Cu}(111)$; i.e., E_{ad} of Ne on the hollow site is lower than that on the atop site. The behavior of E_{ad} of Xe/Cu(111) in the lower panel of Fig. 2(b) is qualitatively different: The atop position is energetically preferred over the hollow site in the same distance range, indicating an *anticorrugated* PES for Xe/Cu(111). Obviously, the opposite corrugation features can be distinguished from PESs of Ne and Xe on Cu(111) in the attractive region. Interestingly, both Ne and Xe have a corrugated PES in the repulsive part, since the hollow site has lower E_{ad} in the magnified view of the E_{ad}–$d_{RG/Cu}(111)$ curves in Fig. 2(c). Here, we zoomed the plots within an energy range that is used in typical helium atom scattering (HAS) experiments (~20–100 meV).

It is interesting that the PES of Xe/Cu(111) undergoes a transition from anticorrugated to corrugated at two "critical" distances, 2.9 Å and 3.8 Å. This suggests that the corrugation feature of Xe/Cu(111) can be changed in different probing distance and energy ranges. In the repulsive region, the RG-substrate interaction is gradually governed by Pauli repulsion.

TABLE I. The interlayer distance, $d_{RG\text{-}Cu(111)}$ (Å), adsorption energy, E_{ad} (meV), and activation energy, E_a (meV), for symmetric structures of Ne/Cu(111) and Xe/Cu(111).

		Ne/Cu(111)		Xe/Cu(111)	
	Site/direction	This work	Ref.	This work	Refs.
E_{ad} (meV)	Top	−50.7	−31.1 [28]	−280.5	−208.1 [28], −250 [12], −269.6 [27], −190 [23]
	Bridge	−51.0	−31.0 [28]	−278.0	−191.2 [28]
	Hollow	−51.0	−31.6 [28]	−277.4	−194.5 [28], −268.6 [27]
$d_{RG/Cu(111)}$ (Å)	Top	3.45	3.57 [28]	3.57	3.36 [28], 3.20 [12], 4.0 [27], 3.60 [23]
	Bridge	3.44	3.60 [28]	3.59	3.41 [28]
	Hollow	3.44	3.59 [28]	3.59	3.42 [28]
E_a (meV)	1	0.28		3.1	
	2	0.26		2.5	

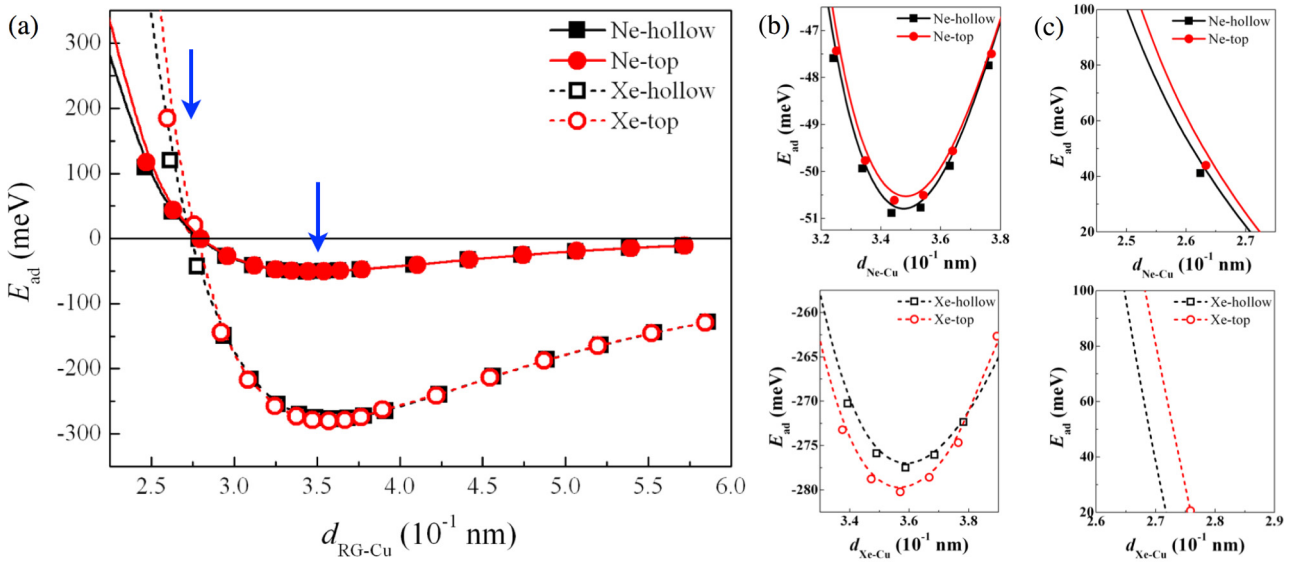

FIG. 2. (Color online) The position and distance dependent adsorption energies of Ne (solid symbols) and Xe (open symbols) on Cu(111). Squares and circles are for energies of RG adatoms on hollow and top sites, respectively. The solid and dashed lines are for eye-guiding purposes. (b) and (c) show the zoom-in plots at the negative and positive adsorption energy regions, as highlighted by the arrows in (a).

Therefore, E_{ad} is typically more positive over the atop site simply because of the shorter interatomic distance in the head-to-head geometry. In the large distance, both Ne and Xe interact with Cu through vdW forces that manifest as the substrate induced charge polarization around RG atoms. It is conceivable that high-coordinate sites (such as hollows) are more favorable.

To see why the PES of Xe/Cu(111) has opposite corrugation behavior from that of Ne/Cu(111) in the intermediate distance range, we show the curves of projected density of states (PDOS) of both systems in their equilibrium geometries in Fig. 3(a). One can see that Ne p states form a sharp peak at -8.6 eV, whereas Xe p states extend in a rather broad energy range around -4.0 eV. In particular, Ne p states have no overlap in energy with Cu d states, so Ne has negligible hybridization with Cu even at a short distance around 3.5 Å. The Xe p states, on the other hand, locate right at the bottom of Cu d bands and thus have a weak hybridization with Cu d orbitals. The energy splitting between Xe $p_{x,y}$ states is obvious in the left inset of Fig. 3(a), an indication of the weak $p_{x,y}$-$d_{xz,yz}$ hybridization at the atop site. The Xe p_z state also intermixes with the Cu $d_z{}^2$ state, but the energy spitting is smaller. Strikingly, small "bumps" appear in the PDOS of Xe/Cu(111) at about $+5.0$ eV above the E_F, as highlighted by the right arrow in Fig. 3(a). This directly suggests the Xe-Cu hybridization and some weak intra-atomic $p \rightarrow s$ charge transfer in Xe. Furthermore, the electron density redistribution of Xe/Cu(111) is notably stronger and extends deeper into the interior Cu layers compared to that of Ne/Cu(111), as discussed in previous studies [28].

To establish the correlation between the anticorrugated PES and the weak p-d hybridization, we also calculated the adsorption of Ne and Xe on Au(111) and Pb(111). We found an anticorrugated PES for Xe on Au(111) in the attractive regime for the same reason elaborated above, but we found corrugated PES for Xe on Pb(111). Both Ne and Xe prefer the hollow site on Pb(111) [17], and their p states form very narrow peaks as shown in Fig. 3(b). We see that Xe p states fall right in the large gap between the s and p states of Pb, while Ne p states have a mismatch in symmetry with the Pb s states, both leading to negligible hybridization between RG and Pb

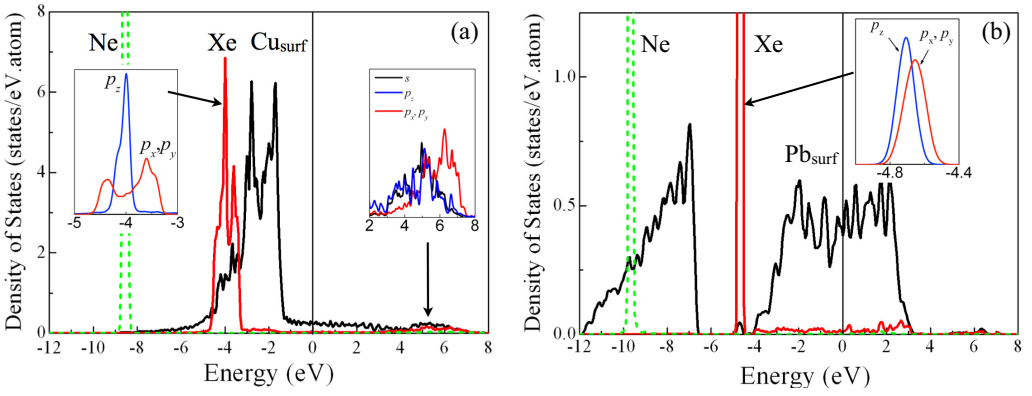

FIG. 3. (Color online) Partial density of states (PDOS) of Ne (green dashed lines), Xe (red/light gray), and the metal atom (black) in the topmost layer of (a) Cu (111) and (b) Pb(111). The insets in (a) display the projected p states of Xe around -4.0 eV (left) and $+5.0$ eV (right) in Xe/Cu(111). The inset in (b) shows the Xe p state around -4.7 eV in Xe/Pb(111). The vertical lines indicate the position of the Fermi level.

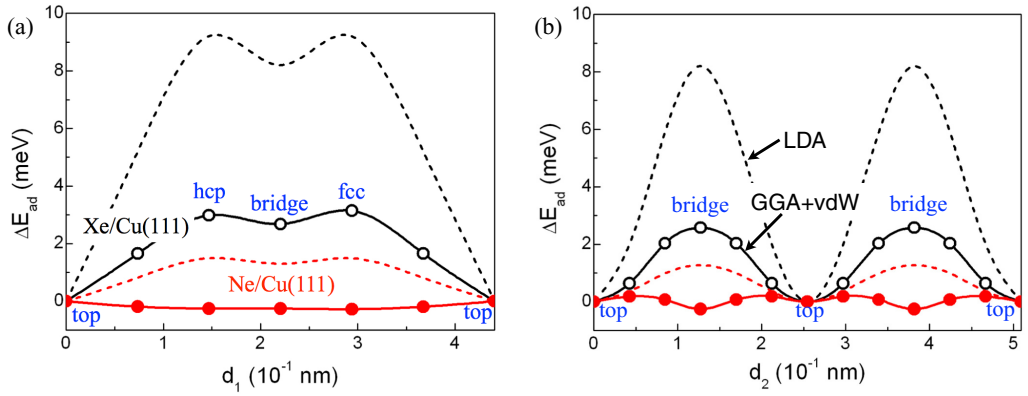

FIG. 4. (Color online) The changes of E_{ad} along (a) path 1 and (b) path 2 shown in Fig. 1: Solid red circles show results for Ne/Cu(111), and open black circles are for Xe/Cu(111). The red and black dashed curves give the LDA results of Ne/Cu(111) and Xe/Cu(111), respectively.

atoms. From these results, we can believe that the Xe-Cu(Au) p-d hybridization is the main reason for the formation of its anticorrugated PES near the equilibrium adsorption distance.

It is worthwhile to point out that the inclusion of the vdW correction in DFT calculations is critical for the correct determination of the corrugation feature of the PESs of RG/Cu(111) and other weak interaction systems [17,29]. In previous studies using the local density approximation (LDA), J. L. F. Da Silva *et al.* [30] concluded that the atop binding of Xe on metal surfaces is a "rule," even on d-lacking surfaces such as Mg(0001) and Al(111). Our results indicate that even Ne/Cu(111) prefers the low-coordination atop geometry if merely the LDA is used, as shown in Fig. 4. In Table I, we listed recent theoretical results for RG/Cu(111) with the inclusion of the vdW term in different versions [12,27,28]. Most structural and energetic parameters are overall consistent and are much improved from LDA results. For example, our data of E_{ad} and $d_{Xe\text{-}Cu(111)}$ are close to results of some previous calculations [27,28], and, particularly, the value of $d_{Xe\text{-}Cu(111)}$ is in good agreement with the experimental value [23]. Nevertheless, discrepancies still exist between different versions and implementations of the vdW correction. For instance, the energy sequence between bridge and hollow sites for Xe/Cu(111) in Ref. [28] is different from ours. Further improvements of the vdW functionals are obviously needed for studies of weak physisorption systems. At this stage, we believe that optB86b version is an appropriate choice for the present system since it gives correct $d_{Xe\text{-}Cu(111)}$ and reasonable E_{ad} for Xe/Cu(111).

It is equally important to study the tribological properties of RG on Cu(111) for applications. There are two possible routes for RG to slide on the Cu(111) surface under the influence of lateral pushing forces: One is along the top → hcp → fcc → top route, and the other is along the top → bridge → top route, as denoted by arrows 1 and 2 in Fig. 1, respectively. We "pushed" the RG adatoms along these two routes and allowed their vertical positions as well as the positions of the topmost five-layer Cu atoms to relax at each step of motion. The segregation energies, defined as $\Delta E_{ad} = E_{ad}^{site} - E_{ad}^{top}$, along paths 1 and 2 are presented in Fig. 4. The activation energies for sliding motion, E_a, can be directly determined from the apexes and valleys of the ΔE_{ad} curves. Due to the corrugated feature of its PES, E_{ad} of Ne/Cu(111) goes down to a lower energy when Ne slides from the atop site to either the hcp site [along route 1 in Fig. 4(a)] or the bridge site [along route 2 in Fig. 4(b)] on Cu(111). On the contrary, pushing Xe away from the atop site along either route 1 or 2 needs to overcome an energy barrier, as shown in Figs. 4(a) and 4(b) with open circles. It is striking to see that values of E_a are very different: 0.28 (0.26) meV for Ne versus 3.1 (2.5) meV for Xe along route 1 (2) through the vdW calculations. From these data, we may estimate that Xe should become movable at around 35 K, which is very close to the experimental result of 50 K by Krim and Widom [31] and Mistura, using the quartz microbalance technique under a high-vacuum condition. On the contrary, Ne can move almost freely on Cu(111), even at a low temperature (∼5 K), because of its small activation energies, a conclusion which is also confirmed by our experimental observations. The dashed lines in Fig. 4 show LDA results [26], which significantly overestimate E_a, 1.27 meV for Ne and 8 meV for Xe. Again, this indicates the need of the vdW correction for the DFT studies of dynamic properties of physisorption systems.

IV. CONCLUSIONS

In summary, we performed self-consistent vdW-DF calculations to study the surface corrugation and tribological properties of Ne and Xe monolayers on Cu(111). Our results show that the potential energy surface is corrugated for Ne/Cu(111) but anticorrugated for Xe near the equilibrium adsorption geometries. The weak hybridization between RG and Cu orbitals is a critical reason for this contrast. For the sliding motion, the activation energy of Ne is noticeably smaller than that of Xe, which leads to a significant difference between their mobilities on Cu(111). From a heuristic point of view, Ne can be an ideal lubricant between two metallic surfaces at a very low temperature. The present work provides an example of using density functional simulations with the van der Waals correction for the understanding of static and dynamic properties of weak physisorption systems.

ACKNOWLEDGMENTS

This work was supported by the Department of Energy-Basic Energy Sciences (DOE-BES) (Grant No. DE-FG02-05ER46237). Calculations were performed on parallel computers at National Energy Research Scientific Computing Center (NERSC).

[1] L. W. Bruch, M. W. Cole, and E. Zaremba, *Physical Adsorption: Forces and Phenomena* (Clarendon, Oxford, 1997).

[2] K. T. Tang and J. Peter Toennies, J. Chem. Phys. **80**, 3726 (1984).

[3] K. H. Rieder, G. Parschau, and B. Burg, Phys. Rev. Lett. **71**, 1059 (1993).

[4] N. Esbjerg and J. K. Nørskov, Phys. Rev. Lett. **45**, 807 (1980).

[5] J. F. Annett and R. Haydock, Phys. Rev. Lett. **53**, 838 (1984).

[6] E. Hulpke, *Helium Atom Scattering from Surfaces* (Springer-Verlag, Heidelberg, 1992).

[7] M. Petersen, S. Wilke, P. Ruggerone, B. Kohler, and M. Scheffler, Phys. Rev. Lett. **76**, 995 (1996).

[8] G. Santoro, A. Franchini, V. Bortolani, D. L. Mills, and R. F. Wallis, Surf. Sci. **478**, 99 (2001).

[9] M. C. Righi and M. Ferrario, Phys. Rev. Lett. **99**, 176101 (2007).

[10] J. L. F. Da Silva and C. Stampfl, Phys. Rev. B **77**, 045401 (2008).

[11] J. Krim, Adv. Phys. **61**, 155 (2012).

[12] P. Lazic, Ž. Crljen, R. Brako, and B. Gumhalter, Phys. Rev. B **72**, 245407 (2005).

[13] M. Rohlfing and T. Bredow, Phys. Rev. Lett. **101**, 266106 (2008).

[14] G. Román-Pérez and J. M. Soler, Phys. Rev. Lett. **103**, 096102 (2009).

[15] P. L. Silvestrelli, Phys. Rev. Lett. **100**, 053002 (2008).

[16] J. Klimeš and A. Michaelides, J. Chem. Phys. **137**, 120901 (2012).

[17] Y. N. Zhang, F. Hanke, V. Bortolani, M. Persson, and R. Q. Wu, Phys. Rev. Lett. **106**, 236103 (2011).

[18] G. Kresse and J. Furthmüller, Comput. Mater. Sci. **6**, 15 (1996).

[19] P. E. Blöchl, Phys. Rev. B **50**, 17953 (1994).

[20] M. Dion, H. Rydberg, E. Schröder, D. C. Langreth, and B. I. Lundqvist, Phys. Rev. Lett. **92**, 246401 (2004); **95**, 109902(E) (2005).

[21] D. C. Langreth, B. I. Lundqvist, S. D. Chakarova-Käck, V. R. Cooper, M. Dion, P. Hyldgaard, A. Kelkkanen, J. Kleis, L. Kong, S. Li, P. G. Moses, E. Murray, A. Puzder, H. Rydberg, E. Schröder, and T. Thonhauser, J. Phys.: Condens. Matter **21**, 084203 (2009).

[22] J. Klimeš, D. R. Bowler, and A. Michaelides, Phys. Rev. B **83**, 195131 (2011).

[23] Th. Seyller, M. Caragiu, R. D. Diehl, P. Kaukasoina, and M. Lindroos, Chem. Phys. Lett. **291**, 567 (1998).

[24] J. L. F. Da Silva, C. Stampfl, and M. Scheffler, Phys. Rev. Lett. **90**, 066104 (2003).

[25] M. C. Righi and M. Ferrario, J. Phys.: Condens. Matter **19**, 305008 (2007).

[26] A. Franchini, V. Bortolani, G. Santoro, and M. Brigazzi, J. Phys.: Condens. Matter **21**, 264008 (2009).

[27] D.-L. Chen, W. A. Al-Saidi, and J. K. Johnson, Phys. Rev. B **84**, 241405(R) (2011).

[28] P. L. Silvestrelli, A. Ambrosetti, S. Grubisiĉ, and F. Ancilotto, Phys. Rev. B **85**, 165405 (2012).

[29] E. Voloshina, Phys. Rev. B **85**, 045444 (2012).

[30] J. L. F. Da Silva, C. Stampfl, and M. Scheffler, Phys. Rev. B **72**, 075424 (2005).

[31] J. Krim, and A. Widom, Phys. Rev. B **38**, 12184 (1988).